Proceedings of the Sixth International Conference on
Railway Technology: Research, Development and Maintenance
Edited by: J. Pombo
Civil-Comp Conferences, Volume 7, Paper 10.1
Civil-Comp Press, Edinburgh, United Kingdom, 2024
ISSN: 2753-3239, doi: 10.4203/ccc.7.10.1

Short-Term Rainfall Prediction Method Considering Orographic Rainfall for the Train Operation Control

Y. Nakabuchi[1], T. Shinomiya[1] and E. Nakakita[2]

[1]Research and Development Center of JR East Group, East Japan Railway Company, Tokyo, Japan
[2]Disaster Prevention Research Institue, Kyoto University

Abstract

To ensure safe train operation in heavy rainfall, railway operators enforce “the train operation control” such as speed reduction and stopping, based on observed precipitation by rain gauges. In the train operation control, trains need to stop immediately when the rainfall value reaches standard values of stop, even if the train is running between stations. When trains stop between stations, it is necessary to stop until rainfall calm down and the surrounding area is confirmed to be safe, and passengers may be kept in the train for a long time. If there is a highly accurate rainfall forecast information, we could know in advance the time when the train operation control will be issued, and stop trains at stations. In this study, as a short-term rainfall prediction method for this objective, we developed a method combining the advection model and the orographic rainfall calculation method. We verified accuracy of predicting the train operation control issuance times by the developed method using multiple rainfall cases. As a result, it was found that in a high probability of about 80% for predictions 10 minutes ahead and about 70% for predictions 20 minutes ahead, the method could predict the issuance time accurately.

Keywords: train operation control, heavy rainfall, train stopping between stations, rainfall prediction, advection model, orographic rainfall calculation method.

1 Introduction

About 75% of Japanese land is mountainous, and there are many railway routes through mountain areas. On these routes, there are many sections consisting of earth structures such as cutting and embankment, and within about 6,200 km local railways of East Japan Railway Company (JR East), about 90% railways are sections of earth structures. In these sections, railway safety can be threatened by slope failures as shown in Figure 1, caused by heavy rain. Slope failures sometimes pose a threat to rail safety. In order to ensure the safety of train operations from slope failures caused by rainfall, railway operators enforce “the train operation control” such as speed reduction and stopping, based on precipitation values observed by rain gauges along railways. In the train operation control, trains need to stop immediately when the amount of rainfall reaches standard values of stop, even if the train is running between stations. When trains stop between stations, it is necessary to stop until rainfall calm down and the surrounding area is confirmed to be safe, and passengers may be kept in the train for a long time. Currently, the train dispatcher guesses the time when rainfall values will reach the standard value of the train operation control, and takes measures to stop the train at a safe station. However, if he makes a mistake, the train may stop between stations in heavy rainfall as shown in Figure 1. Especially on routes in mountain areas, there is a possibility of landslides such as Figure 2. When trains stop between stations in mountain areas, passengers are kept in the train for a long time or there is a risk involved in disasters. In JR East, the train operation controls are issued approximately 200 to 400 times a year, and the train stopping between stations happen about 5 ~ 10 times among them.

Figure 1: Examples of landslides along railway routes in mountain areas.

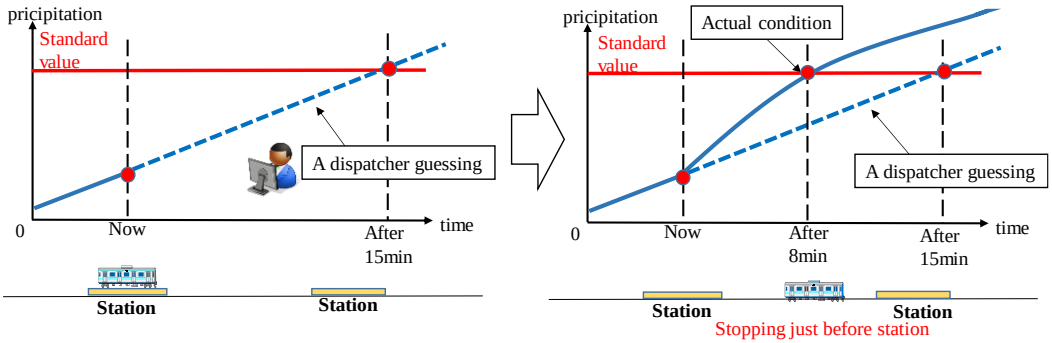

Figure 2: A train stopping between stations when a dispatcher makes a mistake in rainfall guessing.

To prevent the train stopping between stations, we may be able to know in advance the time when the train operation control issue by utilizing rainfall forecast information, and make trains keeping at a station where it is safe and possible to get off. In JR East, almost all distances between the stations is less than 10 km, so on preventing the train stopping between stations, it is sufficient to be able to predict rainfall for a very short period of time, about 10 to 20 minutes ahead. As a suitable method for the short-term rainfall prediction, we developed a method combining the advection model, which is a kinematic prediction method, and a physical model reproducing orographic rainfall in mountain areas. And we also introduced a correction method considering previous prediction errors by comparing prediction rainfall values with observed values of ground rain gauges. In this paper, we describe the details of the developed prediction method and the results of prediction accuracy verification in multiple heavy rainfall events in JR East, and show an availability of the method.

2 Rainfall prediction methods

2.1 Advection model

We use the advection model proposed by Shiiba et al [1] as a core prediction method. In the advection model, a change of the horizontal rainfall intensity distribution $R(x, y)$ is represented by Equation (1). In the spatial coordinate (x, y), the rainfall intensity distribution $R(x, y)$ advects along advection vectors $u(x, y)$, $v(x, y)$ and grow or decay by $\delta(x, y)$.

$$\frac{\partial R(x,y)}{\partial t} + u(x,y)\frac{\partial R(x,y)}{\partial x} + v(x,y)\frac{\partial R(x,y)}{\partial y} = \delta(x,y) \qquad (1)$$

Where the advection vectors $u(x, y)$,$v(x, y)$ in the rain area and the amount of growth-decay rate with time $\delta(x, y)$ are represented as linear Equations (2) at each positions.

$$\begin{aligned} u(x,y) &= c_1 x + c_2 y + c_3 \\ v(x,y) &= c_4 x + c_5 y + c_6 \\ \delta(x,y) &= c_7 x + c_8 y + c_9 \end{aligned} \qquad (2)$$

In Equations (2), c1 to c9 are parameters to be estimated. C1 to c9 can be obtained by solving a linear least squares estimtion problem with Equations (2) based on observation data obtained from time to time. C1 to c9 are updated each time observation data is obtained, and the predicted rainfall intensity distribution is calculated based on the parameters.

In Japan, a radar observation network called XRAIN(eXtended RAdar Information Network) using C-band multi parameter radar and X-band multi parameter radar is maintained by the Ministry of Land, Infrastructure, Transport and Tourism. A 250m mesh rainfall intensity distribution that combines these radar observation values is

called CX composite rainfall data, which is distributed every minute [2]. We calculated predicted values of the advection model every minute, using the CX composite rainfall data every minute as the initial value. For the prediction calculation, we used data of 1 minute intervals up to 5 minutes before the calculation time.

2.2 Orographic rainfall calculation method

The advection model with the CX composite rainfall as an input data has two issues regarding rainfall prediction in mountain areas. The first issue is that the advection model doesn't consider topographical elements, and can't reproduce behavior of rainclouds such as stagnation and growth by influence of topography in mountain areas. The second issue is that in orographic rainfall in mountain areas, the rainfall amounts increases below the observation altitude of radars, so the initial value of CX composite rainfall is tend to less than the value observed by the ground rain gauge [3]. Because of underestimated input data in mountain area, the prediction values tend to be less than the observed values, too.

In order to solve these issues, we utilized a physical-based method reproducing orographic rainfall, proposed by Tatehira [5]. This method considers water vapor condensation caused by air masses rising along mountain slopes, growth of cloud particles themselves, and changes in cloud water content due to conversion to precipitation by the Seeder-Feeder mechanism. If the speed of cloud particles is equal to the speed of air masses, the time change of cloud water amount L [g/m^3] in an air mass is expressed as Equation (3).

$$\frac{dL}{dt} = -cL - a(L - L_c) + WG - WL\left(\frac{\partial \ln \rho}{\partial z}\right) \tag{3}$$

Where ρ_v [g/m^3] is the density of water vapor, c is the ratio of cloud particles captured by raindrops from an upper-level (the Seeder-Feeder mechanism), a is the auto conversion rate from cloud particles to raindrops, L_c [g/m^3] is the threshold of cloud water contents whether the auto conversion happen, W [m/s] is the rising speed of an air mass rising a slope, G [g/m^4] is the amount of increasing L by the water vapor condensation while the air mass rises in a unit distance, and ρ [g/m^3] represents the amount of water vapor. The first and second terms on the right-hand side represent the decrease in cloud water contents due to conversion to precipitation, the third term side represents the condensation of water vapor due to the rise of air masses, and the fourth term represents the change of L due to the compressibility of the atmosphere. The fourth term on the right-hand is one order of magnitude smaller than the third term, so it is ignored. By integrating Equation (3) with respect to time along the flow of air masses, we get Equation (4).

$$L_{\mathrm{out}} = \frac{WG + aL_{\mathrm{c}}}{c + a} + \left(L_{\mathrm{in}} - \frac{WG + aL_{\mathrm{c}}}{c + a}\right) e^{-(c+a)\Delta t} \tag{4}$$

Where L_{out} [g/m^3] is the amount of cloud water contents flowing out of the mesh, L_{in} [g/m^3] is the amount of cloud water contents flowing into the mesh, and Δt [s] is the

time taking for the air mass to pass through one mesh. The orographic rainfall intensity R_O [mm/h] is calculated analytically using Equation (4), considering the balance of L_{in}, L_{out}, and the amount of cloud water contents $WG\Delta t$ condensing and increasing while the air mass passes through the mesh. In Equation (5), H [m] is the layer thickness in which the physical quantities are considered uniform in a vertical direction.

$$R_{\mathrm{O}} = \frac{L_{\mathrm{in}} + WG\Delta t - L_{\mathrm{out}}}{\Delta t} \times 3.6 \times H \tag{5}$$

And we use the method of separating the rainfall intensity R_{radar} [mm/h] obtained from radar rainfall data into the non-orographic rainfall intensity R_N [mm/h] and the orographic rainfall intensity R_O mm/h]. The method was proposed by Nakakita and Terazono [5], and Guimaraes and Nakakita[6] improved it. This method assumes that the R_{radar} is the sum of the R_N and R_O, shown as Equation (6).

$$R_{radar} = R_O + R_N \tag{6}$$

Nakakita and Terazono [5] estimated the nonlinear relationship of Equation (7) between the capture rate c and R_N by fitting those values shown in Tatehira [4].

$$c = 0.6778 R_{\mathrm{N}}^{0.731} \times 10^{-3} \tag{7}$$

By substituting Equation (7) into Equation (4), we obtain the value of L_{out}. And by substituting the value of L_{out} into Equation (5), the R_O can be expressed as a function of the R_N. By combining this equation with equation (6), R_{radar} can be separated into R_O and R_N.

In this study, we applied this method to seven vertical atmospheric layers with constant physical quantities. Using an estimation method similar to that used in Nakakita and Terazono [5], the atmospheric field (wind direction and speed, amounts of water vapor and saturated water vapor) was estimated by interpolating the grid point information to the isobaric surface of 1 km square in the horizontal direction and 15 layers in the vertical direction. The estimated values are used as input data. In addition, as the radar rainfall intensity R_{radar}, we use the CX composite rainfall data, which is regarded as the rainfall data at the 2000m altitude layer.

Figure 3 schematically shows the orographic rainfall calculation method used in this study. For each mesh, the 2000m altitude layer, which is the input layer for the R_{radar}, is the starting point for calculation, and R_N falling from the upper layer is calculated using the separation calculation method described above. For the lower layer, regarding R_{radar} as the R_N for the lower layer, and use this as the input value to calculate the R_O at the lower layer. R_N and R_O of each layer are calculated by repeating these calculations up to the top layer or the bottom layer. As a result, the total rainfall intensity R_T[mm/h] near the ground surface can be estimated as the sum of R_N and R_O (R_{N3} and R_{O3} in Figure 3) at the lowest layer. In this study, we calculate the orographic rainfall at a spatial resolution of 1 km and at calculation intervals of 5 minutes, and the results were used for prediction calculations.

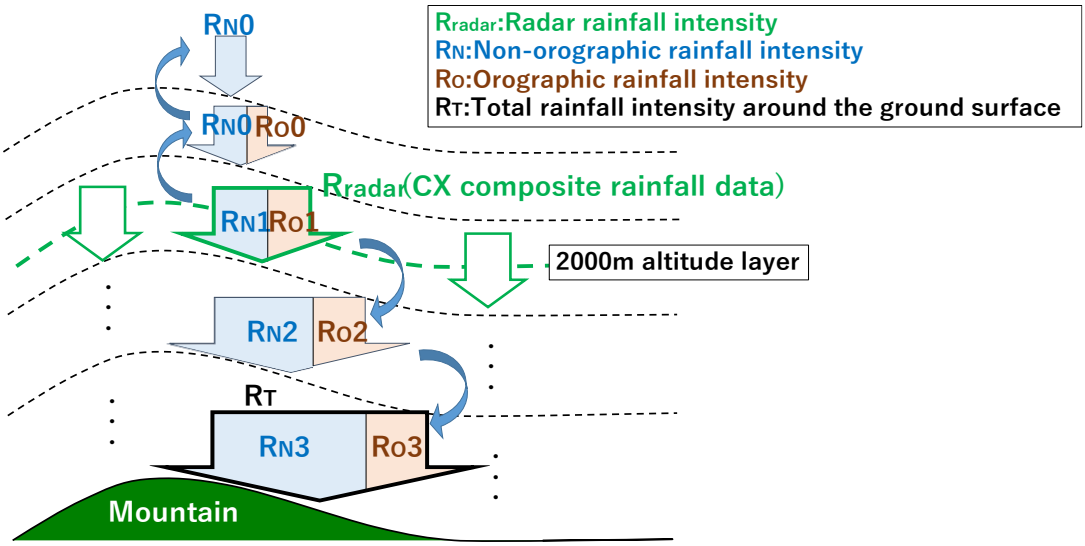

Figure 3: The orographic rainfall calculation method over multiple layers.

2.3 Combining method of the Advection model and the Orographic rainfall calculation method

Figure 4 shows the combining method of the orographic rainfall calculation method and the advection model. We use the non-orographic rainfall intensity R_N (R_{N1} in Figure 3) distributipn separated by the radar input layer in 2.2 as input data of the advection model. First, using the orographic rainfall calculation method, the separated R_N and the orographic rainfall intensity R_O occurring below the radar input layer (sum of R_{O1} to R_{O3} in Figure 3) are calculated every 5 minutes. Next, the R_N distributions for the last 5 minutes is estimated from the CX composite rainfall data every 1 minute using the ratio of R_{radar} and R_N of the orographic rainfall calculation results most recent

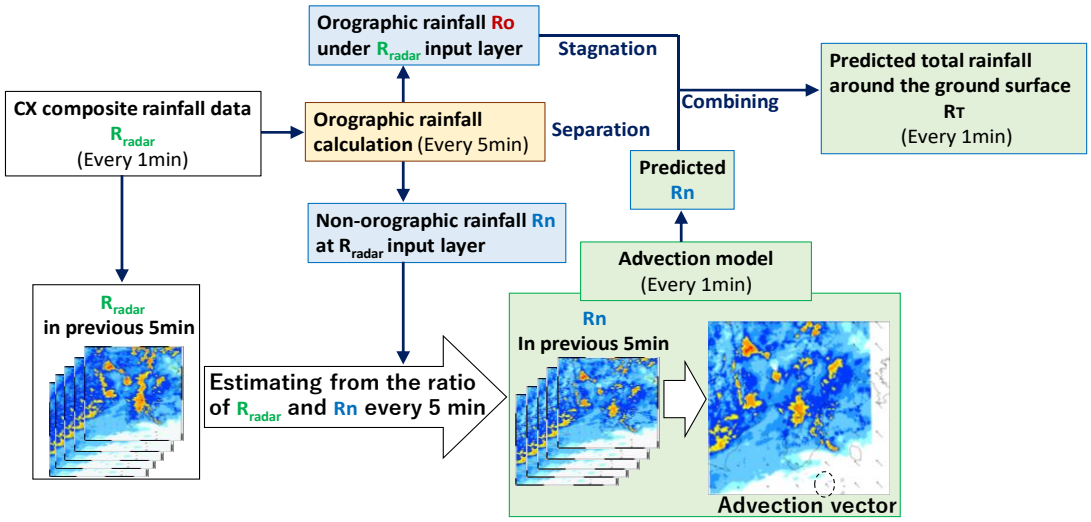

Figure 4: Combining method of the orographic rainfall calculation method and the advection model.

to the calculation time. The R_N distributions for the most recent 5 minutes at the calculation time is regarded as $R(x,y)$ in Equation (1), and the advection vector is estimated. The predicted R_N distribution is calculated by extrapolating the R_N distribution at the calculation time to the predicted time along the advection vector. Since the prediction is for a very short period ahead of time, 10 to 20 minutes ahead, assuming that the R_O distribution will stagnate and remain unchanged from the calculation time, the total rainfall intensity R_T around the ground surface is estimated by combining R_O and predicted R_N at the predicted time.

2.4 Introduction of the error ensemble correction

In this study, in order to increase the prediction accuracy as much as possible, we corrected the predicted values of the method described in 2.3 using "the Error Ensemble" correction method used by Nakakita et al [7]. The error ensemble correction calculates the prediction error at small time intervals up to the calculation time, and determines the statistical properties of the error, and reflects it as a correction amount in the latest predicted value. This method could reduce systematic errors in common in time or space, such as errors caused by rainfall occurring by a generation mechanism which isn't considered in the orographic rainfall calculation method, and errors due to low accuracy of input radar rainfall at the locations far from the weather radar.

Figure 5 shows the method of correcting predicted values using the error ensembles in this study. In the Figure 6, Δt is an interval of prediction calculation (Δt=1 [minutes] in this study), t is the time range using the prediction errors for the correction before the calculation time, and E_n [mm] is the prediction error amounts comparing with rain gauge values at each calculation time. For each calculation time, we calculate all the E_n in the previous t minutes and the average value of them. By adding a correction amount to the predicted value at the calculation time so as to cancel out the average value of the E_n, it is possible to obtain a predicted value that reflects temporal and spatial errors at the time. In this study, we used the error ensemble correction method with t=10 [minutes].

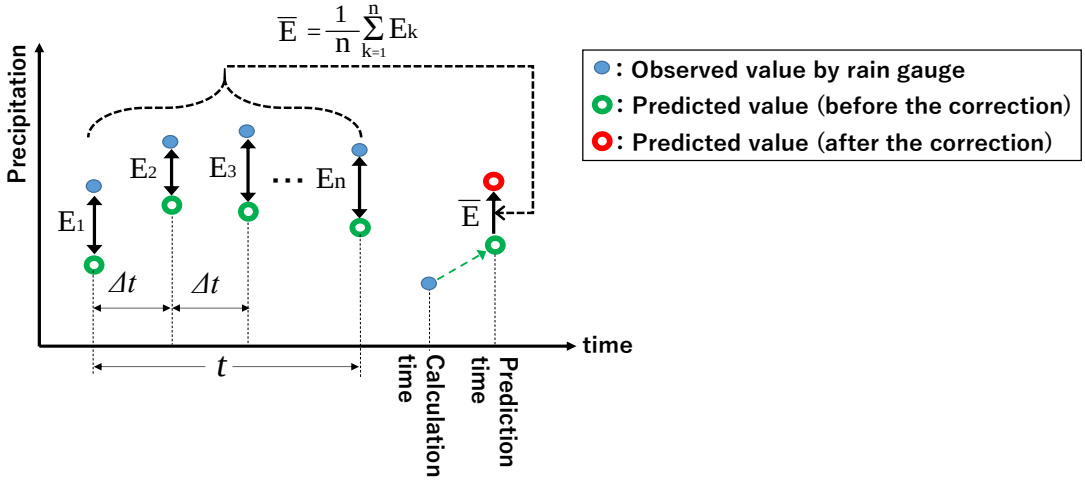

Figure 5: The method of correcting predicted values using the error ensembles.

3 Methodology of verifying prediction accuracy for the train operation control

3.1 Precipitation index in the train operation control

At JR East, the effective precipitation over half-lives of 1.5 hours, 6 hours, and 24 hours are those currently used in reference to the train operation control in heavy rainfall. The effective rainfall is an index which models the amount of water stored in the soil. The standard values are set for each of the three types of the effective rainfall for each rain gauge along the railway. The train operation control is issued when any of the three type effective rainfalls exceed the standard value. Therefore, when verifying the accuracy of predicting the issuance of the train operation control, it is necessary to calculate the effective rainfall value from the predicted rainfall value. The effective rainfall *D(T)* at time *T* is calculated by the following Equation (8), where *D(T-1)* is the effective rainfall value 1unit time ago, *R(T)* is the 1unit hour rainfall at time *T*, *M* is the half-life, and α is the reduction coefficient [8].

$$D(T) = D(T-1)e^{\alpha} + R(T)e^{\frac{\alpha}{2}}$$
$$M = \frac{\ln 0.5}{\alpha} \tag{8}$$

The predicted value of the effective rainfall was calculated by substituting the actual value of the effective rainfall at the calculation time of prediction and the predicted value in 5 minute increments up to the predicted time (20 minutes ahead) into Equation (8).

3.2 Evaluation indices of the prediction accuracy

In verifying the prediction accuracy for the train operation control, we focused on the difference between the time when the observed value exceeds the standard value (actual issuance time) and the time when the predicted value exceeds the standard value (predicted issuance time). Figure 6 shows an image of the actual issuance time and the predicted issuance time. If the predicted issuance time is too late compared to the actual issuance time, the judgment could not be made in time and the train may stop between stations. Also, if the predicted issuance time is too early, we keep the train at station for a long time unnecessarily and take influence to passengers. Therefore, it is desirable that the difference between the predicted issuance time and the actual issuance time is small. Therefore, in this study, we defined a range of the issuance time difference in which the prediction was considered to be correct. Specifically, we defined that the prediction was correct in cases where the predicted issuance time is within the range of 15 minutes before the actual issuance time to 5 minutes after the time. Even if the predicted issuance time is about 15 minutes earlier than the actual issuance time, the influence to passengers may be limited, but if the predicted issuance time is delayed, it will lead to the train stopping between stations, so we set the allowable time short as 5 minutes. We use the two evaluation indices, the capture rate and the hitting rate as shown in Table 1. The capture rate shows a higher value as there are less missing of the actual issuance, so safety can be evaluated.

And the hitting rate shows a higher value as there are fewer miss predicted issuances, so it can be evaluated amounts of the false influence to passengers.

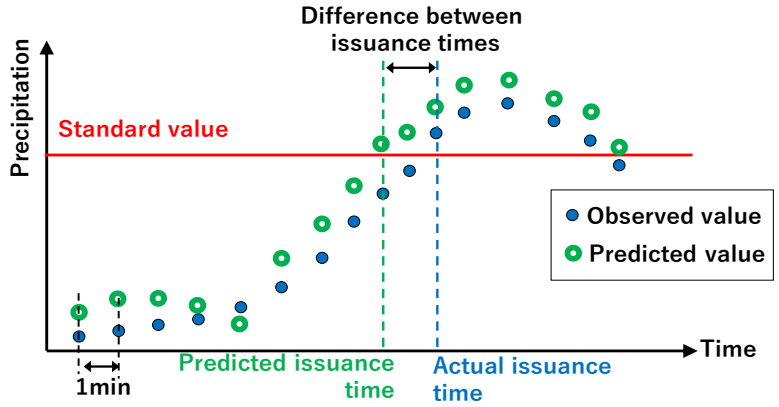

Figure 6: The actual issuance time and the predicted issuance time.

Evaluation index	Definition
Capture rate	$\frac{\text{Number of events (rain gauges) that prediction are correct}}{\text{Number of events (rain gauges) that the observed value reaches the standard value}}$
Hitting rate	$\frac{\text{Number of events (rain gauges) that prediction are correct}}{\text{Number of events (rain gauges) that the predicted value reaches the standard value}}$

Table 1: Definition of the capture rate and the hitting rate.

4 Verification results of prediction accuracy

The prediction accuracy was verified on three cases that have brought heavy rainfall to the east Japan region in recent years, and many rain gauges exceeded the standard values of the train operation control.

4.1 Typhoon Hagibis in October 2019

Typhoon Hagibis in October 2019 landed on the Izu Peninsula with a large and strong force where central pressure was 960 hPa just before 19:00 (JST) on October 12. Typhon Hagibis passed east Japan from south and to north as shown in Figure 7, and the record breaking heavy rains were observed over a wide area at the left of the typhoon's path. By the heavy rainfall of the Hagibis, around JR East railways, landslides occurred in approximately 80 locations, and a few bridges were washed away or vehicles were flooded due to river flooding. In this verification, three areas of approximately 200 km square indicated by blue frames in Figure 8, were set as the calculation areas. The circles shown in Figure 8 indicate railway rain gauges of 307 locations, of which the train operation control issued at 177 rain gauges.

First, in order to confirm the effectiveness of utilizing the orographic rainfall calculation method, we analysed the prediction status of a rain gauge in mountain areas. Figure 9 shows a time series of observed rainfall values and predicted values 20 minutes ahead at Mitake rain gauge in the mountain area of Kanto, around the actual issuance time of the train operation control. The predicted values are two types

of calculation results: one using only the advection model and the other using a combination of the orographic rainfall calculation method and the advection model. In addition, in order to confirm the effectiveness of the model calculation method, the prediction results before applying the error ensemble correction are shown here. The

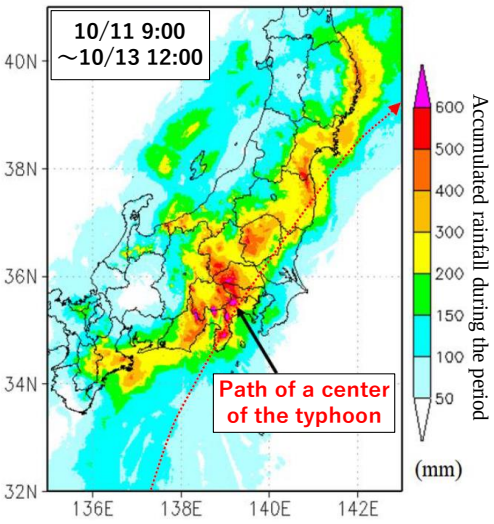

Figure 7: Path of the Hagibis and accumulated rainfall distribution during the passing period (Touch up to press release by the Japan Meteorological Agency [9]).

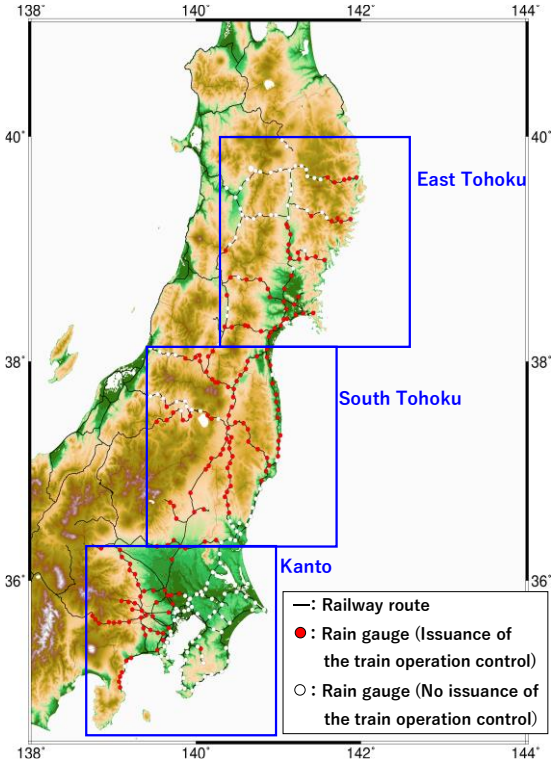

Figure 8: Calculation areas for the Hagibis and rain gauge locations along the railway routes.

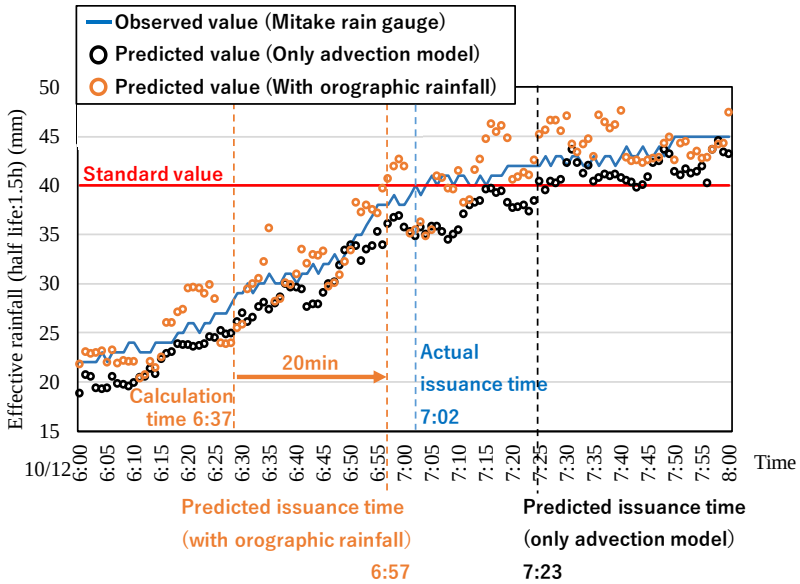

Figure 9: Time series of predicted and observed value at the Mitake rain gauge.

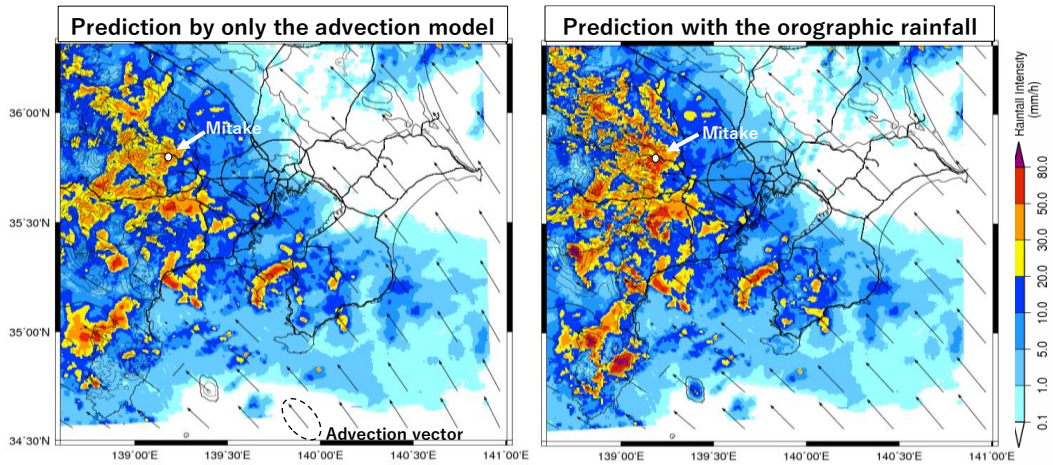

Figure 10: Predicted rainfall distribution 20 minutes ahead at the calculation time 6:37 (Left figure: Prediction result by only the advection model, Right figure: Prediction result with the orographic rainfall calculation method).

predicted values using only the advection model tend to be underestimated than the observed values, and the predicted issuance time was 20 minutes after the actual issuance time. On the other hand, by combining the orographic rainfall estimation method, the underestimation was resolved, and although there was some variation, the predicted values were closer to observed values than the case of only the advection model. As a result, the predicted issuance time was 5 minutes before the actual issuance time, and the prediction was correct. Since the predicted value is calculated before 20 minutes, as shown by the arrow in Figure 9, the possibility of the issuance of the train operation control could be grasped more than 20 minutes before the actual regulation time. Figure 10 shows the predicted rainfall distribution across the Kanto region at 6:57, which is calculated at 6:37 when the prediction value exceeded standard value for the first time by the prediction with the orographic rainfall calculation method. In Figure 10, a location of the Mitake rain gauge is indicated by a circle. In mountain area involving around the Mitake rain gauge, the prediction with the orographic rainfall calculation method shows stronger rainfall than only the advection model. As a result, it is considered that the prediction results were closer to the observed values as shown in Figure 9.

Table 2 shows the results of verifying the prediction accuracy of the developed method of this study, which combines the advection model and the orographic rainfall calculation method, and also introduces the error ensemble correction, targeting the 307 rain gauge locations shown in Figure 8. The predicted value 10 minutes ahead

Evaluation index	10 minutes ahead prediction	20 minutes ahead prediction
Capture rate	81% (143/177)	64% (114/177)
Hitting rate	87% (143/165)	61% (114/157)

Table 2: Capture rate and hitting rate of the prediction method in the Hagibis (The numbers in parentheses represent the number of rain gauges which were sorted to the denominator and the numerator).

shows high prediction accuracy with the capture rate of 81% and the hitting rate of 87%. In addition, although the prediction accuracy decreases slightly, it is good with the capture rate of 64% and the hitting rate of 61% even for predicted values 20 minutes ahead.

4.2 Typhoon Faxai in September 2019

From September 8th to 9th, 2019, the typhoon Faxai brought fierce winds and extremely heavy rainfall to a wide area of the Kanto region, centered on the Boso Peninsula. Figure 11 shows a meteorological satellite infrared image when the Faxai passed. And figure 12 shows the calculation area for this rainfall event. In the area of figure 12, there are 107 rain gauges, and at the 51 rain gauges among them, the train operation control issued.

Table 3 shows the results of verifying the prediction accuracy using the method developed in this study, for the 108 rain gauges shown in Figure 12. The predicted value 10 minutes ahead shows high prediction accuracy with the capture rate of 94% and the hitting rate of 94%. It also shows high prediction accuracy with the capture rate of 75% and the hitting rate of 76% even for predicted values 20 minutes ahead.

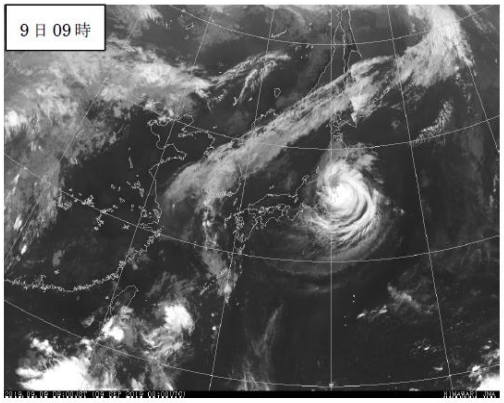

Figure 11: Meteorogical satelite infrared image at 9:00 in September 9th [10].

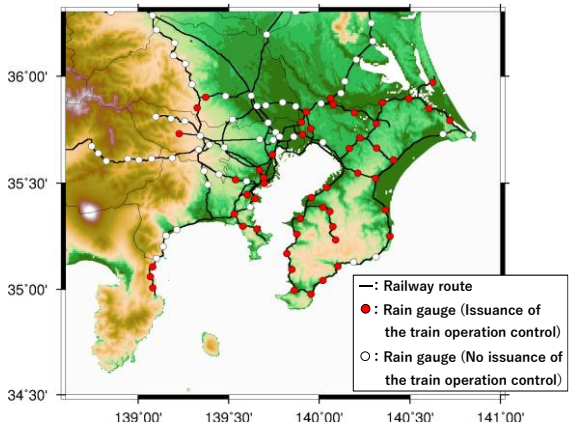

Figure 12: Calculation area for the Faxai and rain gauge locations along the railway routes.

Evaluation index	10 minutes ahead prediction	20 minutes ahead prediction
Capture rate	94% (48/51)	75% (38/51)
Hitting rate	94% (48/51)	76% (38/50)

Table 3: Capture rate and hitting rate of the prediction method in the Faxai (The numbers in parentheses are same as Table 2).

4.3 Seasonal rain front in July 2020

From July 3rd to July 31st, 2020, warm, humid air continued to flow in due to a stationary front near Japan, causing heavy rainfall in various places. In Tohoku region on the Sea of Japan side, this front brought heavy rainfall from July 27th to July 28th.

Figure 13 shows a meteorological satellite infrared image at 9:00 on July 28th. And Figure 14 shows the calculation area for this rainfall event. In the area of Figure 14, there are 88 rain gauges, and at the 27 rain gauges among them, the train operation control issued.

Table 4 shows the results of verifying the prediction accuracy using the method developed in this study, for the 88 rain gauges shown in Figure 14. The predicted value 10 minutes ahead shows high prediction accuracy with the capture rate of 81% and the hitting rate of 88%. In addition, the prediction accuracy for 20 minutes ahead is equivalent to or higher than that for 10 minutes ahead, with the capture rate of 89% and the hitting rate of 92%.

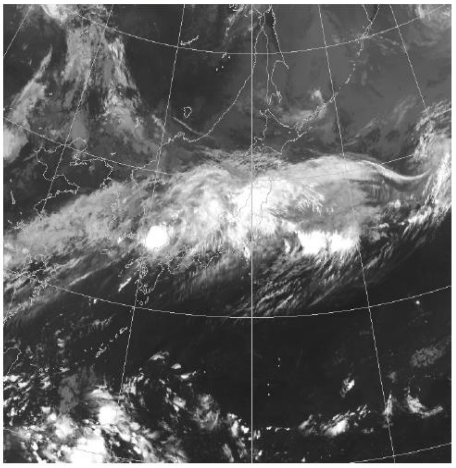

Figure 13: Meteorological satelite infrared image at 9:00 on July 28th [11].

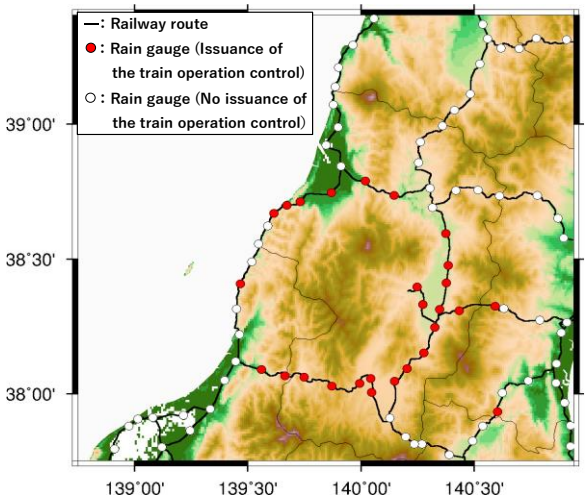

Figure 14: Calculation area for the seasonal rain front and rain gauge locations along the railway routes.

Evaluation index	10 minutes ahead prediction	20 minutes ahead prediction
Capture rate	81% (22/27)	89% (24/27)
Hitting rate	88% (22/25)	92% (24/26)

Table 4: Capture rate and hitting rate of the prediction method in the seasonal rain front (The numbers in parentheses are same as Table 2).

5 Conclusion

In this study, we investigated the use of a short-term rainfall prediction method to prevent the train stopping between stations when the train operation control is issued. We developed the prediction method combining an advection model and the orographic rainfall calculation method, and also introducing the error ensemble correction. To verify the prediction accuracy of the method, we focused on the prediction accuracy of the issuance time of the train operation control. As a result of verifying for three heavy rainfall cases, it was found that in a high probability of about 80% for predictions 10 minutes ahead and about 70% for predictions 20 minutes ahead, the method could predict the train operation control issuance time accurately.

In JR East, almost all distances between the stations is less than 10 km, so if we grasp that the train operation control will be issued 10 to 20 minutes in advance, we could generally prevent the trains stopping between stations.

We will further verify the accuracy in other cases in order to improve the reliability of the method. Furthermore, we will proceed the study aim to introduce the method to the train operation, for example we let the train dispatchers use the prediction method at the train operation control rooms by way of experiment.

References

[1] Shiiba, M., Takasao, T. and Nakakita, E., "Investigation of short-term rainfall prediction method by a translation model", Proceedings of the Japanese Conference on Hy-draulicsisaster, Vol.28, 423-428, 1984.

[2] Foudation of River & basin Integrated Communications, "Composit method of the radar rainfall data", www.river.or.jp/post_24.html.

[3] Mizuta, N., Takenaka, H., Sano, T. and Fukami, K. "Approach to accuracy improvement of rainfall intensity observed by multi-parameter radars in XRAIN of MLIT", Proceedings of the Foudation of River & basin Integrated Communications symposium, 2021.

[4] Tatehira, R., "Orographic rainfall computation including cloud-precipitation interaction", Tenki, Vlo.23, No.2, pp.27-32, 1976.

[5] Nakakita, E., Terazono, M., "A short-term rainfall pre-diction taking into consideration nonlinear effect of non-orographic rainfall on orographic rainfall", Journal of japan Society of Civil Enginieers, Hydroulic engineering, Vol.52, 331-336, 2008.

[6] Guimaraes, G., Nakakita, E., "Verification by Full Volume Scan Radar Observation of Vertical Rainfall Profile Estimated by an Orographic Rainfall Model Based on the Seeder-Feeder Mechanism", Proceedings of Disaster Prevention Research Institute Annual Meeting, C208, 2021.

[7] Nakakita, E., Yoshikai, T, and Sunmin, K., "Application of Error-Ensemble prediction method to a short-term rainfall prediction model considering orographic rainfall", Weather Radar and Hydrology (Proceedings of a symposium held in Exeter, UK, April 2011) (IAHS Publ, 351), 317-322, 2012.

[8] Suzuki, M. and Kobashi, S., "The critical rainfall for the disasters caused by slope failure", Journal of the Japan Society of Erosion Control Engineering, Vol.121, 16-25, 1981.

[9] Japan weather agency press release, "Factors of heavy rainfall in the typhoon Hagibis on 2019", 2019.

[10] Choshi local Meteorological Observatory, "Chiba Prefecture weather report regarding Typhoon No. 15 on 2019", https://www.data.jma.go.jp/obd/bsdb/data/files/sg_history/12000/2019/12000_2019_1_10_1.pdf, 2019.

[11] Japan weather agency, "Weather cases that caused disasters - Heavy rainfall in July 2020 -", https://www.data.jma.go.jp/obd/stats/data/bosai/report/2020/20200811/jyun_sokuji20200703-0731.pdf, 2020.